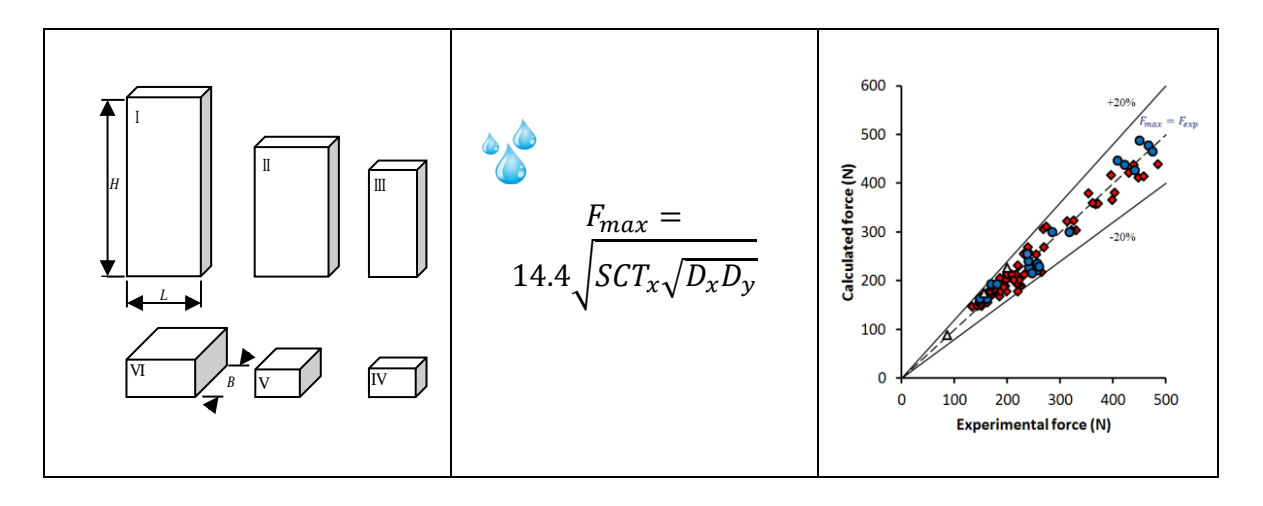
Optimization of the Solid Cardboard in Carton Design

Yuriy Pyr'yev,^a Katarzyna Piłczyńska,^{a,*} Edmundas Kibirkštis,^b Laura Gegeckienė,^b Ingrida Venytė,^b and Kęstutis Vaitasius ^b

*Corresponding author: katarzyna.pilczynska@pw.edu.pl

DOI: 10.15376/biores.19.4.7963-7976

GRAPHICAL ABSTRACT



Optimization of the Solid Cardboard in Carton Design

Yuriy Pyr'yev,^a Katarzyna Piłczyńska,^{a,*} Edmundas Kibirkštis,^b Laura Gegeckienė,^b Ingrida Venytė,^b and Kęstutis Vaitasius ^b

The present research aimed to increase the accuracy of predicting the maximum force required to compress a solid cardboard box. Changes in the technology of solid cardboard production and the design of packaging help to increase the durability of packaging; however, typical estimation methods do not take these changes into account. By determining the number of important parameters of the box and using a specific approach, it was possible to develop a semiempirical model of the maximum force that compresses the box and simplifies its description. By using this model, the amount of solid board required for a specific package can be reduced without reducing the life of the box. The maximum force prediction method is also suitable for creating other box models at different moisture levels.

DOI: 10.15376/biores.19.4.7963-7976

Keywords: Paperboard cartons; Solid cardboard; Strength; Maximum compression force; Moisture

Contact information: a: Department of Printing Technologies, Faculty of Mechanical and Industrial Engineering, Warsaw University of Technology, Konwiktorska 2, 00-217 Warsaw, Poland; b: Department of Production Engineering, Faculty of Mechanical Engineering and Design, Kaunas University of Technology, Studentų 56, 51424 Kaunas, Lithuania;

* Corresponding author: katarzyna.pilczynska@pw.edu.pl

INTRODUCTION

The packaging market is an extremely important branch of industry, with an estimated global value of over USD 199 billion in 2023. Food packaging accounts for almost USD 340 billion (Walsh 2023). Therefore, improving the quality of boxes is important for the industry. It is also important to implement ecological solutions, and this trend includes the use of cardboard packaging and limiting the use of plastics. In addition, attention is given to the carbon footprint generated by the paper industry. The use of lighter cardboard produced under compliance to environmental standards contributes to this reduction. The use of lighter cardboard is possible, especially when the products have very good parameters, including stiffness and mechanical strength.

As part of the research, the mechanical strength of the cardboard packaging was checked, and the results of the McKee formula, *i.e.*, the method of estimating the static strength of solid cardboard boxes, were verified. To date, models have been developed mainly for corrugated cardboard, while for solid cardboard, the literature describing a McKee-type model has been significantly limited (Kibirkstis *et al.* 2007; Pyryev *et al.* 2016, 2019).

The elastic buckling of panels for estimating the compressive strength of a corrugated box was considered in a pioneering work (McKee *et al.* 1963). The estimate depends on parameters describing the compressive strength and bending stiffness of the box panels and parameters determined empirically. A similar expression was later derived for cardboard boxes in the work of Grangård and Kubát (1969) and Grangård (1970).

The solid paperboard containers described in the article are the unit packaging for individual items, while the corrugated containers protect goods during transport. They are subject to various loads that affect the safety of the products being transported. Bivainis and Jankauskas' paper described puncture resistance tests (2015), while only Johst *et al.* (2023) considered the effect of kinetic energy. Multiple-Impact-Test-Rig experiments were used for this purpose. This test method is based on a compressor and a velocity sensor. The experiment observed damage phenomena such as imprint, cracking, and breakthrough.

An interesting study was also carried out by Cornaggia *et al.* (2023), who examined the effect of relative humidity and temperature on bending, compression, and stiffness of corrugated board. It was a numerical investigation, which enabled the authors to create a comprehensive map of the correlation between the change in humidity of cardboard layers and the strength characteristics of this paper product.

A series of models for determining the compressive strength of a corrugated box was studied, and the errors in the measurement input data of these models were propagated to estimate the uncertainty in the predicted values. A brief analysis of the role of artificial intelligence in revolutionizing both corrugated board production and corrugated packaging design is given in Frank and Kruger's study (2021).

The paper by Garbowski *et al.* (2020) presents analytical methods for estimating the top-to-bottom static compressive strength of simple corrugated packaging, taking into account the torsional and shear stiffness of corrugated board and the depth-to-width ratio of the panel. A brief analysis of the role of artificial intelligence in revolutionizing both corrugated board production and corrugated packaging design is provided in Garbowski's study (2024).

In the study by Ristinmaa *et al.* (2012), analytical expressions were developed to predict the *BCT* strength of cardboard boxes by analyzing the deformation of panels and corner panels. The deformation and damage of the panels at failure are determined by the yield lines, which represent the folds that develop during testing. The geometry of the yield lines depends on the geometry of the box. A panel with a low aspect ratio relative to width will have different yield lines than a panel with a high aspect ratio. Yield lines often extend from the corners into the panel. Their work established that during *BCT*, a large part of the load will be taken by the corners of the panels. At the maximum load, the corner area will collapse, which is not a stability problem but rather a purely plastic mechanism where the cardboard is crushed or delaminated. Therefore, the *BCT* test activates several deformation and damage mechanisms before failure. In a box with a rectangular cross-section, the corners will take a large part of the load, which is due to the buckling of the sidewalls.

Packages of this size are often used for packing cereal products such as rice, which are additionally packed separately (Kibirkštis *et al.* 2007).

In the study by Pyryev *et al.* (2022), a semiempirical model of the maximum compressive force of solid cardboard boxes (BCTs) was proposed,

$$F_{max} = 15.2 \times SCT_x^{0.49} \left(\sqrt{D_x D_y} \right)^{0.51} P^{-0.020} (P/H)^{0.329}$$
 (1)

where F_{max} is the maximum compression force (N) (vertical maximum force in the x direction); D_x and D_y are the flexural rigidities in the x and y directions (N m); P = 2(L+B) is the perimeter of the rectangular plate $L \times B$ (m); H is the height of the carton (m); and SCT_x is the compressive strength in the x direction of the board using a short-span compressive tester (N/m).

Based on the work of Ristinmaa et al. (2012) and Marin et al. (2021), the proposed

semiempirical models have been tested on independent experimental data to predict the compressive force of a carton. Physical experiments by Marin *et al.* (2021) were performed at 50%, 70%, and 90% relative humidity (RH).

This work proposes a corrected semiempirical model for predicting the maximum compressive force of a solid cardboard box based on the following formula (Eq. 1).

EXPERIMENTAL

Data and Materials

Six different types of cardboard packaging designs were used to create the engineering calculation procedure for the maximum compression force (Kibirkštis *et al.* 2007; Pyryev *et al.* 2022). This article proposes new models and compares them with older models for predicting the compressive strength from the top to the bottom of folded cardboard boxes. In these works, the compression data of 72 cardboard boxes were analyzed (i = 1, ..., 72) (Fig. 1a): six cardboard boxes with different geometric parameters, six different types of cardboard compressed in the cross direction (CD) (Fig. 1b), and six in the machine direction (MD) (Fig. 1c). There were six test repetitions for each of the 72 boxes. The geometric parameters of the carton boxes are summarized in Table 1.

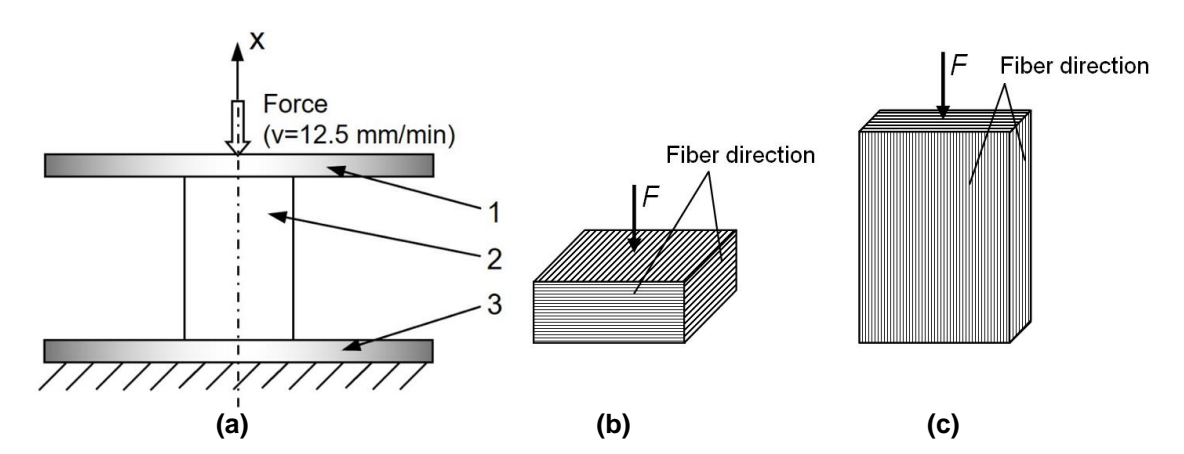


Fig. 1. Compression testing scheme for a package under the action of vertical force F and (N) of the load: (a) principal scheme, (b) compression testing scheme in the cross direction (CD), (c) compression testing scheme in the machine direction (MD), 1) moving base support: v = 12.5 mm/min, 2) package under compression, and 3) fixed base support.

A simplified diagram of the pressing station and a view of the packaging samples are shown in Figs. 1 and 2. This type of boxed cardboard was chosen for the experiment because of its popularity in the food packaging industry. For the cardboard boxes with dimensions shown in Fig. 2a (i = 1, 2, ..., 36), some experimental data, such as the cardboard strength and compression strength at a short span, and the bending stiffness of the cardboard were previously presented by the authors in earlier articles (Kibirkštis *et al.* 2007; Pyryev *et al.* 2016). The experimental data for the compression tests of carton packs were obtained in a standard atmosphere for conditioning and testing in accordance with the requirements of ISO 187 (2022). Low cartons were also tested for additional analysis (Fig. 2b). Pyryev *et al.* (2022) presented experimental data for 36 boxes (Fig. 2b) (i = 37..., 72). Research with the low paper board in Fig. 2b was carried out with the same type of boards as for the boards in Fig. 2a.

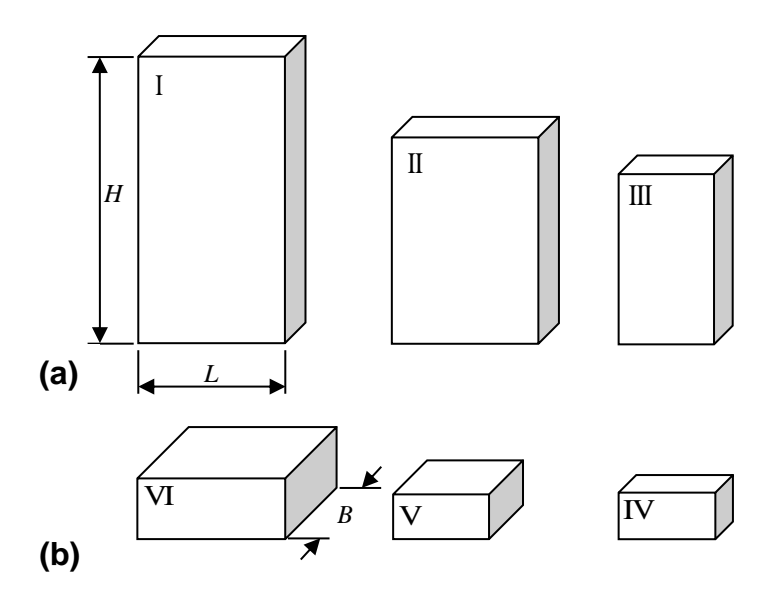


Fig. 2. The geometric parameters of the packaging specimen

Table 1. Geometric Parameters of the Packaging Specimen

| | Carton size (Pyryev et al. 2022) | | | | | | | Carto inmaa | Carton size (Marin et al. 2021) | | |
|--------------|----------------------------------|---------------------|------|------|------|-----------------|-----|----------------|---------------------------------------|-----|-----|
| | I | Ш | III | IV | V | VI | VII | VIII | XI | | |
| L (mm) | 118 | 118 | 77 | 77 | 77 | 118 | 150 | 150 | 150 | 150 | 40 |
| B (mm) | 48 | 48 | 37 | 37 | 77 | 118 40 50 50 50 | | | 50 | 40 | |
| H(mm) | 230 | 165 | 137 | 37 | 37 | 48 | 200 | 50 | 100 | 200 | 80 |
| P=2(L+B)(mm) | 332 | 332 332 228 228 308 | | 472 | 380 | 400 | 400 | 400 | 160 | | |
| λ=P/H (-) | 1.44 | 2.01 | 1.66 | 6.16 | 8.32 | 9.83 | 1.9 | 8.0 | 4.0 | 2.0 | 2.0 |

Compressive Strength Test

The compressive strength test involves placing cardboard between rigid plates that compress it at the deformation rate recommended by ISO 12048 (1994) (12.5 mm/min). The DBBMTOL-500 N sensor (serial number AP34282) was used. The accuracy of the load measurements was \pm 0.5%, indicating that the load ranged from 2% to 100%. Other parameters include the accuracy of measurement position (\pm 0.01% of reading or 0.001 mm) and accuracy of speed (\pm 0.005% of set speed). The maximum force of load that the sample can withstand was measured as the compression force $F_{\rm exp}$. This value is experimental. The most important technical parameters of boards are compressive strength (SCT) and bending stiffness (D). The box samples used in the experiment are described in Fig. 2. For the carton parameter $\lambda = P/H$.

The mentioned boxes were made from different boards: (1) Soft MC Mirabell paperboard (WLC) or (GD2) – Recycled Coated White Lined Chipboard; (2) Kromopak paperboard (FBB) or (GC2) – Folding Boxboard; (3) Korsnas Carry (SUB) or (GN4) – Solid Unbleached Board; and (4) Korsnas Light (SUB) or (GN4) – Solid Unbleached Board. The boxes were constructed according to the No A60.20.00.03 PackDesign 2000 Standard Libraries for ECMA.

| No | Type of paperboard | Grammage ISO 536 (2019) (g/m²) | SO 536 ISO 534 (2019) (2011) | | Bending fness 5°), (mNm) 28 (2019) | SCT = Compressive strength, (kN/m) ISO 9895 (2008) | | |
|----|---------------------|---|---------------------------------|--------|---|--|--------|--|
| | | | | MD^2 | CD^3 | MD^2 | CD^3 | |
| 1 | MC Mirabell (WLC) | 400 | 565 | 60.9 | 24.4 | 12.7 | 8.5 | |
| 2 | MC Mirabell (WLC) | 320 | 435 | 31.8 | 13.3 | 9.8 | 7.4 | |
| 3 | Kromopak (FBB) | 300 | 430 | 34.3 | 14.3 | 9.2 | 6.8 | |
| 4 | Kromopak (FBB) | 275 | 395 | 29.0 | 12.0 | 8.6 | 6.2 | |
| 5 | Korsnas Carry (SUB) | 400 | 585 | 113.0 | 55.3 | 11.2 | 8.4 | |
| 6 | Korsnas Light (SUB) | 290 | 420 | 41.9 | 21.2 | 8.5 | 6.1 | |

Table 2. Comparison of Paperboard Technical Characteristics (Kibirkštis *et al.* 2007)

The technical data of the cardboard are presented in Table 2. In terms of their characteristics, two directions of the fibers are distinguished: the machine direction (MD) and the cross direction (CD). The first is generally preferred because it follows the direction of the machine. However, for the purposes of the experiment, to compare the theoretical properties, two directions of the fibers were considered.

The results were also compared with those previously described by Kibirkštis (for reference to boards, see Fig. 2a). To predict the compressive force of the board, semiempirical models were tested during the experiment.

Modeling the Compressive Strength

First, there is a contact problem with the nonlinear theory of plasticity and elasticity of anisotropic material structures. This is important for determining the maximum compression force of the carton. The area of plasticity and the contact load on the side panels of the board are unknown. Owing to the semiempirical approach and the numerical method proposed by Pyr'yev (2019, 2022), it is possible to solve this problem.

$$F_{max} = aK \left(D_x/D_y\right)^b \left(SCT_y/SCT_x\right)^c \left(P_{ef}/H\right)^d, \ K = \sqrt{SCT_x\sqrt{D_xD_y}} \eqno(2)$$

where a, b, c, and d are constant parameters defined on the basis of experimental data; $P_{ef} = 16S/P = 8LB/(L+B)$; and $S = L \times B$. Introducing the effective perimeter $P_{ef} = 4((B^2 + L^2) / 2)^{1/2}$, as in (Coffin 2015), did not yield the best result. The model is called semiempirical because of the use in (2) of the K-factor obtained, for example, by Grangård (1970) and Pyryev *et al.* (2019).

Applying the logarithm functions to the right and left parts of Eq. 2, one obtains:

$$\ln\left(F_{max}/K\right) = \ln\left(a\right) + b\ln\left(D_x/D_y\right) + c\ln\left(SCT_y/SCT_x\right) + d\ln\left(P_{ef}/H\right) \quad (3)$$

Previous equation can be written as follows:

$$\tilde{y} = b_0 + b_1 x_1 + b_2 x_2 + b_3 x_3 \tag{4}$$

¹L&W device-measured moment needed for bending the sample material to an angle of 5°

²MD - machine direction

³CD - cross machine direction

where

$$\tilde{y} = \ln(F_{max}/K), b_0 = \ln(a), b_1 = b, b_2 = c, b_3 = d$$
 (5)

$$x_1 = \ln(D_x/D_y), x_2 = \ln(SCT_y/SCT_x), x_3 = \ln(P_{ef}/H)$$
 (6)

By knowing the constant coefficients b_0 , b_1 , b_2 , and b_3 in Eq. 4, the a, b, c, and d values can be written in Eq. 2:

$$a = e^{b_0}, b = b_1, c = b_2, d = b_3$$
 (7)

Calculation of the Multiple Linear Regression Coefficients

The measurement data and the coefficients of the model are represented in matrix form,

$$\mathbf{y} = \begin{bmatrix} y_1 \\ \vdots \\ y_n \end{bmatrix}, \mathbf{X} = \begin{bmatrix} 1 & x_{1,1} & x_{1,2} & x_{1,3} \\ \vdots & \vdots & \vdots & \vdots \\ 1 & x_{n,1} & x_{n,1} & x_{n,3} \end{bmatrix}, \mathbf{b} = \begin{bmatrix} b_0 \\ \vdots \\ b_3 \end{bmatrix}, \mathbf{e} = \begin{bmatrix} e_1 \\ \vdots \\ e_n \end{bmatrix}, \ \tilde{\mathbf{y}} = \mathbf{X}\mathbf{b}, \ n = 72 \quad (8)$$

where y is the measurement vector column for measuring the compression force, $y_i = \ln(F_{exp}^i/K^i)$; $K^i = \left(SCT_x^i\right)^{0.5}(D_x^iD_y^i)^{0.25}$; **X** is the dimension matrix $n \times 4$, in which the i-th row i = 1, 2, ..., n represents the i-th observation of the vector of independent variable values x_1, x_2, x_3 values corresponding to the variables at given free term b_0 ; **b** – vector-column of dimension 4 parameters of the multiple regression equation; **e** – vector-column of dimension n of deviations $e_i = y_i - \tilde{y}_i$ where y_i depends on \tilde{y}_i obtained from the regression equation:

$$\tilde{y}_i = b_0 + b_1 x_{i,1} + b_2 x_{i,2} + b_3 x_{i,3}, i = 1, 2, ..., n, \quad \tilde{\mathbf{y}} = \mathbf{Xb},$$
 (9)

where $x_{i,1} = \ln(D_x^i/D_y^i), x_{i,2} = \ln(SCT_y^i/SCT_x^i), x_{i,3} = \ln(P_{ef}^i/H^i)$

The matrix form of the relation is:

$$\mathbf{e} = \mathbf{y} - \mathbf{X}\mathbf{b} \tag{10}$$

According to the least squares method,

$$\sum_{i=1}^{n} e_i^2 = \mathbf{e}^T \mathbf{e} = (\mathbf{y} - \mathbf{X}\mathbf{b})^T (\mathbf{y} - \mathbf{X}\mathbf{b}) \to min, \tag{11}$$

where $e^T = (e_1, ..., e_n)$, *i.e.*, the superscript T indicates a transpose matrix. It may be shown that the previous condition is fulfilled if the vector-column of coefficient b can be obtained by the following formula,

$$\mathbf{b} = (\mathbf{X}^T \mathbf{X})^{-1} \mathbf{X}^T \mathbf{y} \tag{12}$$

$$R^{2} = 1 - \frac{\sum_{i=1}^{n} (y_{i} - \tilde{y}_{i})^{2}}{\sum_{i=1}^{n} (y_{i} - \bar{y})^{2}}$$
(13)

where the determination coefficient R² is the average value of the dependent variable.

$$\bar{y} = \frac{1}{n} \sum_{i=1}^{n} y_i \tag{14}$$

The model is based on experiments with different mechanical and geometrical dimensions of packages (72 different cartons). The model is also valid for cartons with other parameters within the parameter range studied in the present paper.

RESULTS AND DISCUSSION

Box Compression Strength – Experiment

The experimental findings and the parameters of the cartons under testing are presented in Table A. The experimentally obtained values for the maximum force of compression F_{exp} are shown in column 5 of Table A (Pyryev *et al.* 2022). For example, the first experiment (i = 1) obtained the following: mean carton compression strength, 329 N; maximum, 344 N; minimum, 315 N; standard deviation, 11 N; and coefficient of variation, 3.29%.

The analysis of the data presented in Tables 1 and 2 allows us to determine the range of nondimensional parameters: $SCT_x / SCT_y \in [1.0; 2.08]$; $D_x / D_y \in [0.52; 9.42]$; $B / H \in [0.2; 2.5]$; $L / H \in [0.51; 8.6]$; $\lambda = P / H \in [1.44; 9.80]$.

Experiment vs. Model for the Maximum Compression Force

In this study, n = 72. Based on the findings of the experiment, the coefficients of linear regression in Eq. 4 can be evaluated using the least squares method: $b_0 = 2.62375$, $b_1 = 0.1149$, $b_2 = 0.2859$, $b_3 = 0.02855$. The multiple coefficient of correlation (Eq. 13) between the dependent variable and the explanatory parameters is R = 0.974943.

In accordance with Eq. 7, the following constant values are found: a = 13.79, b = 0.1149, c = 0.2859, and d = 0.02855.

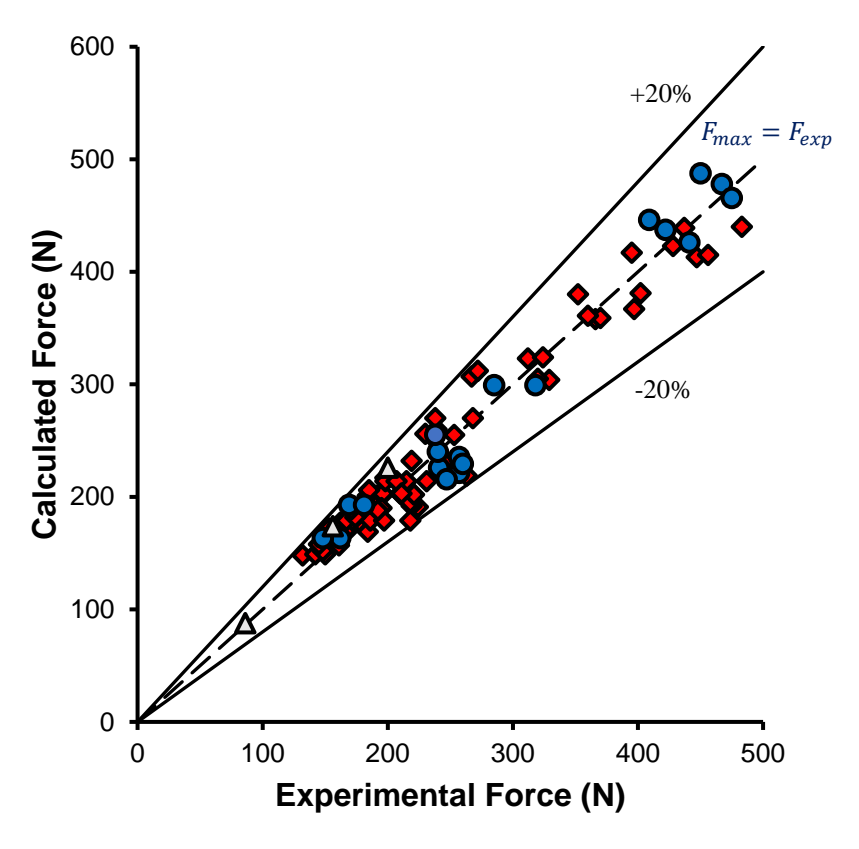


Fig. 3. The maximum compression force for the packaging F_{max} (Eq. 15) was predicted *via* comparison with the experimental data F_{exp} (Pyryev *et al.* 2022), which is represented by diamonds. Data from Ristinmaa *et al.* (2012) is represented in circles, and data from Marin *et al.* (2021) is represented in triangles.

The following mathematical model was developed based on the experimental findings:

$$F_{max} = 13.79 \times K(D_x/D_y)^{0.1149} (SCT_y/SCT_x)^{0.2859} (P_{ef}/H)^{0.02855}$$
(15)

By entering the data from Table A into Eq. 15, the values of the maximum compression force were calculated (Table A, column 6).

The average deviation of the calculated values F_{max}^{i} from the experimental data F_{exp}^{i} (i = 1, ..., 72), was determined by the following formula:

$$MAPE = \frac{100}{n} \sum_{i=1}^{n} \varepsilon_i, \ \varepsilon_i = \frac{|F_{exp}^i - F_{max}^i|}{F_{exp}^i}$$
 (16)

The MAPE (mean absolute percentage error) was found to be 6.41%.

A comparison of the predicted forces (Table A, column 6) and experimental failure forces (Table A, column 5) is shown in Fig. 3, with diamonds representing the experimental data (Pyryev *et al.* 2022), revealing a close correlation.

The line $F_{max} = F_{exp}$ represents the calculated maximum force (Eq. 15), while the lines + 20% and - 20% indicate the area with the absolute value of the relative error $\varepsilon_i < 0.2$, and cover at least 80% of the obtained values, respectively.

When the quality of the effective length in the formula (Eq. 15) is represented by $P_{ef} = 4((B^2 + L^2) / 2)^{1/2}$ in Coffin (2015), the parameters are a = 13.67, b = 0.1149, c = 0.2859, d = 0.03174, and the MAPE = 6.44019%.

If the quality of the effective length considers the perimeter of the package $P_{ef} = 2(B + L)$, the parameters are a = 13.70, b = 0.1149, c = 0.2859, d = 0.03077, and MAPE = 7.75%.

Simplified Model for the Maximum Compression Force

The small values of the dimensionless parameters b, c, and d in Eq. 15 provide a basis for writing the formula for the maximum compressive force of the packaging in the form,

$$F_{max} = 14.4 \sqrt{SCT_x \sqrt{D_x D_y}} \tag{17}$$

which does not depend on geometric parameters, a = 14.4, and MAPE = 7.11%.

With the packaging parameters used, Eq. 17 can assess the compressive strength of cuboid packaging.

Model Tested for the Maximum Compression Force

The proposed semiempirical prediction models for the maximum compressive force of a cardboard box were tested based on the experimental results (Ristinmaa *et al.* 2012).

The experimental results are presented for three different materials and four different box sizes (Table 1), as well as for two types: A1111 (i = 1, ...16) and A6020 (i = 17, ...20), according to the ECMA classification (Table A in Pyr'yev 2022). The bending resistance values, BR_{MD} , BR_{CD} (mN), (ISO 2493) SCT_{MD} , and SCT_{CD} (mN/m) are also presented in Table A (Pyr'yev *et al.* 2022).

The comparison results are shown in Fig. 3 with circles, revealing a close correlation, with a MAPE of 6.95%

Model for the Maximum Compression Force and Humidity

The obtained formulas (Eqs. 15 and Eq. 17) can be used for predictions, including variations in the moisture content of packages. Testing of the proposed semiempirical predictive models for the maximum compressive force of a cardboard box was based on experimental results (Marin *et al.* 2021). The paperboard used in this study was a commercial multi-fold paperboard with kraft pulp in the outer layers and a mixture of chemical-thermomechanical pulp (CTMP), kraft pulp, and a cracked middle layer. The grammage was 260 g/ m², density was 764 kg/ m³, and plate thickness was h = 0.34 mm. Physical experiments were performed at relative humidity levels of 50%, 70%, and 90% at 23 °C. Linear relationships between the mechanical properties of the paperboard and moisture were obtained. Poisson's in-plane coefficients were assumed to follow the equation (v_{xy} , v_{yx}) $^{0.5} \approx 0.293$ (Marin *et al.* 2021).

The material inputs used in the simulations are given in Table 3, which contains the measured values at 50%, 70%, and 90% RH (relative humidity). The parameters from Table 3 were converted into bending stiffness parameters D_x , D_y , and crushing stiffness parameters SCT_x , SCT_y

$$D_x = \frac{E_x h^3}{12(1 - \nu_{xy} \nu_{yx})}, D_y = \frac{E_y h^3}{12(1 - \nu_{xy} \nu_{yx})}, SCT_x = \sigma_x h, SCT_y = \sigma_y h$$
 (18)

Table 3. Experimental Data for Paperboard Package Compression Tests for Predicting of the Maximum Compression Force and Corresponding Error (Marin *et al.* 2021)

| | The | RH(%) | Емд | Ecd | σ_{MD} | σ_{CD} | F _{exp} | F _{max} | 100 ε _i | F _{max} | 100 ε _i |
|----|--|-------|-----|-----|---------------|---------------|------------------|------------------|--------------------|------------------|--------------------|
| | box | | GPa | GPa | MPa | MPa | (N) | (N) | (%) | (N) | (%) |
| | design | | | | | | (Marin | based | based | based | based |
| | type | | | | | | et al. | on | on | on | on |
| | Tab. 2 | | | | | | 2021) | Eq.15 | Eq.16 | Eq.17 | Eq.16 |
| 1 | 2 | 3 | 4 | 5 | 6 | 7 | 8 | 9 | 10 | 11 | 12 |
| 1 | XI | 50 | 5.8 | 3.0 | 59 | 35 | 200 | 226 | 13.1 | 238 | 19.2 |
| 2 | XI | 70 | 4.7 | 2.4 | 43 | 26 | 156 | 254 | 11.8 | 260 | 17.2 |
| 3 | XI | 90 | 2.8 | 1.4 | 18 | 11 | 86 | 87.8 | 2.05 | 91.8 | 6.70 |
| ۸h | Abbreviation: RH, relative humidity; σ_{MD} , σ_{CD} , short-span compression. | | | | | | | | | | |

The comparison results are shown in Fig. 3 with triangles, revealing a close correlation between the predicted forces (Table 3, column 10) and the experimental failure forces (Table A, column 8)

Potential Industrial Applications

The packaging industry is a very important branch of the economy that continues to grow. Packaging manufacturers are looking for solutions that enable more cost-effective production while maintaining the best quality boxes. The research presented in this article has shown that it is possible to use cardboard with a lower grammage without losing strength properties. The solution presented is both economical and safe for the packaged product. The use of packaging with good strength properties contributes to reduced logistics costs as well as improved shelf life. Furthermore, the resulting empirical field pattern can be used in the design and manufacture of a solid board box

CONCLUSIONS

- 1. A formula for predicting the maximum compression force of a solid cardboard box has been developed. The formula can be used for different moisture content values.
- 2. A four-parameter theoretical model (Eq. 15) and a one-parameter model (Eq. 17) for the maximum compression force were developed and analyzed to determine the compression effect of the paperboard packaging.
- 3. For the experimental data presented in the paper, the model (Eq. 15) yields a *MAPE* of 6.41%.
- 4. A comparison between the theoretical (Eq. 15) and experimental results shows sufficient accuracy.
- 5. The semiempirical formula (Eq. 17) for predicting the compression force of the carton with a MAPE = 7.11 is noteworthy. The formula has a simple shape and does not depend on the geometric parameters of the carton, including the height of the carton H. As a first approximation, a new Eq. 17 is used.
- 6. The proposed models (Eq. 15) were successfully tested on 20 independent experimental data points (Pyryev *et al.* 2021; Ristinmaa *et al.* 2012), with an average error of 6.95% and a *MAPE* of 7.35% (Eq. 17).
- 7. The proposed models (Eq. 15) were successfully tested on 3 independent experimental data points (Marin *et al.* 2021) at relative humidity levels of 50%, 70%, and 90%.
- 8. The theoretical model (Eq. 15) allows the prediction of the carton's height if the expected load F_{max} is known,

$$H = P_{ef} \left(13.79 K \left(D_x / D_y \right)^{0.1149} \left(SCT_y / SCT_x \right)^{0.2859} / F_{max} \right)^{33.33}$$
 (19)

9. If the expected force F_{max} of the carton is indicated, a cardboard with a predicted compressive strength SCT_x can be chosen according to Eq. 17,

$$SCT_x = (F_{max}/14.4)^2/\sqrt{D_x D_y}$$
 (20)

10. The developed simplified semiempirical models allow for the optimization of the design of cuboidal packaging with sufficient accuracy.

ACKNOWLEDGMENTS

The authors are grateful for the support of the European Union in the framework of European Social Fund (POKL 04.01.01-00-002/08-01) through the Warsaw University of Technology Development Programme.

REFERENCES CITED

Bivainis, V., and Jankauskas, V. (2015). "Impact of corrugated paperboard structure on puncture resistance," *Materials Science* 21(1), 37-61. DOI: 10.5755/j01.ms.21.1.5713

- Coffin, D.W. (2015). "Some observations towards improved predictive models for box compression strength," *TAPPI Journal* 14(8), 537-545. DOI: 10.32964/TJ14.8.537
- Cornaggia, A., Gajewski, T., Knitter-Piątkowska, A., and Garbowski, T. (2023). "Influence of humidity and temperature on mechanical properties of corrugated board Numerical investigation," *BioResources* 18(4), 7490-7509. DOI: 10.15376/biores.18.4.7490-7509
- Frank, B., and Kruger, K. (2021). "Assessing variation in package modeling," *TAPPI Journal* 20(4), 231-238. DOI: 10.32964/TJ20.4.231
- Garbowski, T. (2024). "Revolutionizing corrugated board production and optimization with artificial intelligence," *BioResources* 19(2), 2003-2006. DOI: 10.15376/biores.19.2.2003-2006
- Garbowski, T., Gajewski, T., and Knitter-Piątkowska, A. (2022). "Influence of analog and digital crease lines on mechanical parameters of corrugated board and packaging," *Sensors* 22, article 4800, 1-19. DOI: 10.3390/s22134800
- Garbowski, T., Gajewski, T., and Grabski, J. K. (2020). "The role of buckling in the estimation of compressive strength of corrugated cardboard boxes," *Materials* 13(20), 4578. DOI: 10.3390/ma13204578
- Grangård, H. (1970). "Compression of board cartons. 1. Correlation between actual tests and empirical equations," *Svensk Papperstidning-Nordisk Cellulosa* 73(15), article 462.
- Grangård, H., and Kubát, J. (1969). "Some aspects of the compressive strength of cartons," *Svensk Papperstidning-Nordisk Cellulosa* 72(15), 466-473.
- ISO 12048 (1994). "Packaging Complete, filled transport packages Compression and stacking tests using a compression tester," International Organization for Standardization. Geneva, Switzerland.
- ISO 187 (2022). "Paper, board and pulps Standard atmosphere for conditioning and testing and procedure for monitoring the atmosphere and conditioning of samples," International Organization for Standardization. Geneva, Switzerland.
- ISO 534 (2011). "Paper and board Determination of thickness, density and specific volume," International Organization for Standardization. Geneva, Switzerland.
- ISO 536 (2019). "Paper and board Determination of grammage," International Organization for Standardization. Geneva, Switzerland.
- ISO 5628 (2019). "Paper and board Determination of bending stiffness General principles for two-point, three-point and four-point methods", International Organization for Standardization. Geneva, Switzerland.
- ISO 9895 (2008). "Paper and board Compressive strength Short-span test," International Organization for Standardization. Geneva, Switzerland.
- Johst, P., Kaeppeler, U., Seibert, D., Kucher, M., and Böhm, R. (2023). "Investigation of different cardboard materials under impact loads," *BioResources* 18(1), 1933-1947. DOI: 10.15376/biores.18.1.1933-1947
- Kibirkštis, E., Lebedys, A., Kabelkaitė, A., and Havenko, S. (2007). "Experimental study of paperboard package resistance to compression," *Mechanika* 63(1), 27-33.
- Marin, G., Srinivasa, P., Nygårdsa, M., and Östlund, S. (2021). "Experimental and finite element simulated box compression tests on paperboard packages at different moisture levels," *Engineering Packaging Technology and Science* 34(4), 229-243. DOI: 10.1002/pts.2554
- McKee, R. C., Gander J. W., and Wachuta J. R. (1963). "Compression strength formula for corrugated boxes," *Paperboard Packaging* 48(8), 149-159.

- PackDesign 2000. Standard Libraries for ECMA, BCSI Systems BV, Hoeven, The Netherlands (2000)
- Pyr'yev, Y., Kibirkštis, E., Gegeckienė, L., Vaitasius, K., and Venytė, I. (2022). "Empirical models for prediction compression strength of paperboard carton," *Wood and Fiber Science* 54(1), 60-73. DOI: 10.22382/wfs-2022-06
- Pyryev, Y., Kibirkštis, E., Miliūnas, V., and Sidaravičius, J. (2016). "Engineering calculation procedure of critical compressive force of paperboard packages," *Przeglad Papierniczy* 72(6), 374-381. DOI: 10.15199/54.2016.6.1
- Pyryev, Y., Zwierzyński, T., Kibirkštis, E., Gegeckienė, L., and Vaitasius, K. (2019). "Model to predict the top-to-bottom compressive strength of folding cartons," *Nordic Pulp & Paper Research Journal* 34(1), 117-127. DOI: 10.1515/npprj-2018-0032
- Ristinmaa, M., Ottosen, N.S., and Korin, C. (2012). "Analytical prediction of package collapse loads Basic considerations," *Nordic Pulp & Paper Research Journal* 27(4), 806-813. DOI: 10.3183/npprj-2012-27-04-p806-813
- Walsh, S. (2023). "The future of folding cartons to 2028," (https://www.smithers.com/engb/resources/2023/may/smithers-forecasts-growth-folding-carton-market), Accessed 22 June 2023.

Article submitted: July 29, 2024; Peer review completed: August 18, 2024; Revised version received and accepted: August 24, 2024; Published: September 3, 2024. DOI: 10.15376/biores.19.4.7963-7976

APPENDIX

Table A. Experimental Data for Paperboard Package Compression Tests for Predicting of the Maximum Compression Force and Corresponding Error

| | The | | | | _ | | _ | |
|----|----------|-------------|-----------|------------------|------------------|----------------|------------------|----------------|
| | | Type of | Load | F _{exp} | F _{max} | 100 ε <i>i</i> | F _{max} | 100 ε <i>i</i> |
| | box | paperboard, | direction | (N) | (N) | (%) | (N) | . (%) |
| | design | No. | | | based on | based | based | based |
| | type | | | | Eq.15 | on | on | on |
| | Fig. 2 | | | _ | | Eq.16 | Eq.17 | Eq.16 |
| 1 | 2 | 3 | 4 | 5 | 6 | 7 | 8 | 9 |
| 1 | ! | 1 | MD | 329±11 | 304 | 7.60 | 318 | 3.25 |
| 2 | | 1 | CD | 235±6 | 254 | 8.09 | 260 | 10.8 |
| 3 | <u> </u> | 2 | MD | 191±5 | 201 | 5.24 | 204 | 6.92 |
| 4 | l | 2 | CD | 164±5 | 168 | 2.44 | 177 | 8.21 |
| 5 | II | 1 | MD | 320±6 | 305 | 4.69 | 318 | 0.53 |
| 6 | II | 1 | CD | 253±3 | 255 | 0.79 | 260 | 2.92 |
| 7 | II | 2 | MD | 211±2 | 202 | 4.27 | 204 | 3.21 |
| 8 | II | 2 | CD | 167±3 | 169 | 1.20 | 177 | 6.27 |
| 9 | Ш | 1 | MD | 267±12 | 307 | 15.0 | 318 | 19.2 |
| 10 | Ш | 1 | CD | 230±8 | 256 | 11.3 | 260 | 13.2 |
| 11 | III | 2 | MD | 210±7 | 203 | 3.33 | 204 | 2.75 |
| 12 | III | 2 | CD | 161±4 | 169 | 4.97 | 177 | 10.2 |
| 13 | | 3 | MD | 184±3 | 201 | 9.24 | 205 | 11.6 |
| 14 | I | 3 | CD | 165±2 | 168 | 1.82 | 177 | 6.99 |
| 15 | | 4 | MD | 162±3 | 177 | 9.26 | 182 | 12.5 |
| 16 | | 4 | CD | 132±8 | 148 | 12.1 | 155 | 17.2 |
| 17 | II | 3 | MD | 196±3 | 202 | 3.06 | 205 | 4.77 |
| 18 | II | 3 | CD | 184±3 | 169 | 8.15 | 177 | 4.06 |
| 19 | II | 4 | MD | 177±2 | 178 | 0.56 | 182 | 2.94 |
| 20 | II | 4 | CD | 150±1 | 149 | 0.67 | 155 | 3.14 |
| 21 | Ш | 3 | MD | 196±2 | 203 | 3.57 | 205 | 4.77 |
| 22 | Ш | 3 | CD | 167±4 | 170 | 1.80 | 177 | 5.71 |
| 23 | Ш | 4 | MD | 186±4 | 179 | 3.76 | 182 | 2.04 |
| 24 | III | 4 | CD | 142±1 | 149 | 4.93 | 155 | 8.95 |
| 25 | | 5 | MD | 447±2 | 413 | 7.61 | 428 | 4.24 |
| 26 | | 5 | CD | 366±3 | 358 | 2.19 | 371 | 1.28 |
| 27 | II | 5 | MD | 456±3 | 415 | 9.00 | 428 | 6.13 |
| 28 | II | 5 | CD | 370±5 | 359 | 2.97 | 371 | 0.19 |
| 29 | III | 5 | MD | 395±6 | 417 | 5.57 | 428 | 8.36 |
| 30 | III | 5 | CD | 360±5 | 361 | 0.28 | 371 | 2.97 |
| 31 | | 6 | MD | 198±7 | 217 | 9.60 | 229 | 15.6 |
| 32 | I | 6 | CD | 195±6 | 190 | 2.56 | 194 | 0.53 |
| 33 | II | 6 | MD | 246±9 | 218 | 11.4 | 229 | 6.92 |
| 34 | II | 6 | CD | 224±8 | 191 | 14.7 | 194 | 13.4 |
| 35 | III | 6 | MD | 263±7 | 219 | 16.7 | 229 | 12.9 |
| 36 | III | 6 | CD | 219±9 | 192 | 12.3 | 194 | 11.4 |
| 37 | IV | 1 | MD | 272±7 | 312 | 14.7 | 318 | 17.0 |
| 38 | IV | 1 | CD | 239±8 | 260 | 8.79 | 260 | 8.95 |
| 39 | V | 1 | MD | 312±7 | 323 | 3.53 | 318 | 2.02 |
| 40 | V | 1 | CD | 268±6 | 270 | 0.75 | 260 | 2.84 |
| 41 | VI | 1 | MD | 324±5 | 324 | 0.00 | 318 | 1.76 |
| 42 | VI | 1 | CD | 238±5 | 270 | 13.4 | 260 | 9.41 |
| 43 | IV | 2 | MD | 217±4 | 206 | 5.07 | 204 | 5.89 |
| 44 | IV | 2 | CD | 168±5 | 172 | 2.38 | 177 | 5.63 |

| | | | | , | 1 | | | |
|----|----------|---|----|-------|-----|------|-----|------|
| 45 | V | 2 | MD | 215±6 | 214 | 0.47 | 204 | 5.01 |
| 46 | V | 2 | CD | 172±7 | 179 | 4.07 | 177 | 3.18 |
| 47 | VI | 2 | MD | 198±8 | 214 | 8.08 | 204 | 3.14 |
| 48 | VI | 2 | CD | 167±9 | 179 | 7.19 | 177 | 6.27 |
| 49 | IV | 3 | MD | 185±4 | 206 | 11.4 | 205 | 11.0 |
| 50 | IV | 3 | CD | 153±8 | 172 | 12.4 | 177 | 15.4 |
| 51 | V | 3 | MD | 207±1 | 214 | 3.38 | 205 | 0.80 |
| 52 | V | 3 | CD | 197±2 | 179 | 9.14 | 177 | 10.4 |
| 53 | VI | 3 | MD | 231±9 | 214 | 7.36 | 205 | 11.1 |
| 54 | VI | 3 | CD | 218±9 | 179 | 17.9 | 177 | 19.0 |
| 55 | IV | 4 | MD | 174±5 | 182 | 4.60 | 182 | 4.72 |
| 56 | IV | 4 | CD | 148±7 | 152 | 2.70 | 155 | 4.53 |
| 57 | V | 4 | MD | 192±1 | 188 | 2.08 | 182 | 5.10 |
| 58 | V | 4 | CD | 161±2 | 157 | 2.48 | 155 | 3.91 |
| 59 | VI | 4 | MD | 171±1 | 189 | 10.5 | 182 | 6.55 |
| 60 | VI | 4 | CD | 145±2 | 158 | 8.97 | 155 | 6.70 |
| 61 | IV | 5 | MD | 428±7 | 423 | 1.17 | 428 | 0.01 |
| 62 | IV | 5 | CD | 397±5 | 367 | 7.56 | 371 | 6.63 |
| 63 | V | 5 | MD | 437±8 | 439 | 0.46 | 428 | 2.05 |
| 64 | V | 5 | CD | 352±7 | 380 | 7.95 | 371 | 5.31 |
| 65 | VI | 5 | MD | 483±9 | 440 | 8.90 | 428 | 11.4 |
| 66 | VI | 5 | CD | 402±5 | 381 | 5.22 | 371 | 7.79 |
| 67 | IV | 6 | MD | 253±4 | 223 | 11.9 | 229 | 9.50 |
| 68 | IV | 6 | CD | 218±5 | 195 | 10.6 | 194 | 11.0 |
| 69 | V | 6 | MD | 245±5 | 231 | 5.71 | 229 | 6.54 |
| 70 | V | 6 | CD | 221±8 | 202 | 8.60 | 194 | 12.2 |
| 71 | VI | 6 | MD | 219±7 | 232 | 5.93 | 229 | 4.55 |
| 72 | VI | 6 | CD | 211±7 | 203 | 3.79 | 194 | 8.07 |